JOURNAL OF THERMOPHYSICS AND HEAT TRANSFER
Vol. 21, No. 3, July–September 2007

Experimental Verification of Thermal Switch Effectiveness in Thermoelectric Energy Harvesting

R. McCarty*
University of Dayton, Dayton, Ohio 45469
D. Monaghan†
U.S. Air Force Research Laboratories, Air Vehicles Directorate, Wright–Patterson Air Force Base, Ohio 45433
K. P. Hallinan‡
University of Dayton, Dayton, Ohio 45469
and
B. Sanders§
U.S. Air Force Research Laboratories, Air Vehicles Directorate, Wright–Patterson Air Force Base, Ohio 45433

DOI: 10.2514/1.27842

This paper presents research seeking to experimentally verify the effectiveness of a thermal switch used in series with thermoelectric devices for waste heat recovery for constant and variable source heat input and for variable source thermal capacitance (mass). Using an experimental setup composed serially of a fixed heat source, a variable thermal resistance air gap serving as a thermal switch, a thermoelectric device, and a heat sink, the time-averaged power output to power input ratios improved up to 15% and 30%, respectively, for constant and variable heat input in certain design space conditions. The experimental results, as supported by model predictions, suggest that the thermal capacitance of the heat source must be greater than the thermal capacitance of the thermoelectric device in order for thermal switching to improve the time-averaged power output to power input ratios of waste heat recovery systems. The results have direct application to aircraft energy harvesting.

Nomenclature

C	=	thermal capacitance (J/kg · K
f	=	frequency, Hz
k	=	thermal conductivity, W/mK
P	=	output power from TE device, W
PR	=	output power to input power ratio, %
Q	=	heat dissipation, W
R	=	thermal resistance, K · m^2/W
S	=	Seebeck coefficient
T	=	temperature, °C
T	=	period, s
t	=	time, s
W	=	work, W
x	=	spatial coordinate, m
ZT	=	thermoelectric device figure of merit
ΔT	=	temperature change, °C
ρ	=	resistivity, Ωm
Φ	=	electrochemical potential, eV

Subscripts

H	=	hot side of the thermoelectric device
in	=	input into system
L	=	cold side of the thermoelectric device
max	=	maximum
Mounting	=	mounting resistance which includes ceramic plates, epoxy, and contact resistance
nc	=	no control
off	=	thermal resistance setting when thermal switch is open
on	=	thermal resistance setting when thermal switch is closed
out	=	output from system
p	=	thermal switch
s	=	heat source
sink	=	heat sink
steady	=	steady state
switching	=	power ratio with source temperature control
TE	=	thermoelectric device

I. Introduction

THE thermoelectric effect or the ability of a material to convert a temperature difference into electric power is driven by the Seebeck coefficient which is given by Eq. (1), [1],

$$S = \frac{-\mathrm{d}\Phi/\mathrm{d}x}{\mathrm{d}T/\mathrm{d}x} \tag{1}$$

The Seebeck coefficient is included in a thermoelectric (TE) figure of merit, ZT, defined as

$$ZT = \frac{S^2 T}{\rho k} \tag{2}$$

Recently breakthrough developments in thermoelectric devices have been reported showing increases in the ZT value for TE device materials from 1 up to 5 [2–4]. Bell [5] illustrated that surpassing the threshold ZT of 2 in a cost effective manner can enable significant usage of TE energy harvesting to convert waste heat in an automobile

Received 15 September 2006; revision received 1 December 2006; accepted for publication 1 December 2006.

*Graduate Research Assistant, Mechanical and Aerospace Engineering, 300 College Park.
†Deputy Team Lead, AFRL/VAS, 2210 Eighth Street.
‡Chair and Professor, Mechanical and Aerospace Engineering, 300 College Park.
§Team Lead, AFRL/VAS, 2210 Eighth Street. AIAA Associate Member.

engine exhaust into electrical power. Recently, Fairbanks [6] noted that further improvements in ZT to approximately 10 could make TE power conversion competitive with the internal combustion engine. Finally, Elder et al. [7] stated that for automotive applications, TE utilization is possible if the module cost is brought down to approximately 0.10/W and a ZT value above 3 can be achieved over a broad temperature range.

Relative to aircraft energy harvesting from power electronics, Hallinan and Sanders [8] showed that TE technology is already at a state where a positive system level impact can be realized.

Transient behavior of the thermal-electrical energy conversion processes in TE devices for use in heat pumps has received some attention [9–13]. As a cooler, the TE device instantly adsorbs electric energy at the p–n junctions when current is applied. Simultaneously, Joule heating results, but this thermal energy diffuses toward the p–n junction at a much slower rate than the electron flow. As a result, the Seebeck effect is enhanced, and therefore the TE device performance is temporarily improved until the Joule heating effects reach steady state. When the TE device operates as a generator, Joule heating diffusion begins at the p–n junction when a temperature difference is applied across the device. Electrical energy adsorption commences almost instantaneously, thus temporarily degrading the Seebeck effect and the TE device performance until Joule heating reaches steady state. For a typical bismuth telluride TE device, the transient effects occur for very small time durations on the order of 0.2 s, substantially lower than the time periods considered here; therefore transient TE behavior is assumed to be negligible.

The waste heat recovery system with thermal switch source temperature modulation, shown schematically in Fig. 1, is proposed to harvest waste heat from a constant or variable heat source using TE devices. In this figure, each layer has defined thermal resistances and capacitances. The mounting resistance layer on either side of the TE device includes the thermal resistance of the ceramic material sandwiching the active thermoelectric elements, high thermal conductivity epoxy applied to both surfaces of the TE device, and the contact resistance.

As an illustration of a typical energy harvesting system with no thermal switching, Fig. 2 shows source temperatures and power dissipation plotted as a function of time. Also noted is the maximum allowable source temperature of 160°C. In practice, this system must be designed for worst case heat input scenarios due to variations in source heat output, sink temperature and thermal resistance, and manufacturing. This conservative design can force the system to at times operate well below the maximum temperature of the source, therefore reducing the temperature drop across the TE device and thus lowering the efficiency of the system. To compensate for these variations, the representative waste heat recovery system shown in Fig. 3 is proposed to maximize the thermoelectric energy recovery from the system through the addition of a thermal switch, located between the source and the TE device. Again, in this illustration of a typical energy harvesting system, source temperature and power into the TE device are plotted as a function of time. The thermal switch has controllable thermal resistance. As shown in the representative plot, when the heat input is near maximum, the thermal resistance of the thermal switch is set to a minimum to prevent the source from exceeding its maximum temperature. In this state the heat flows freely into the TE device, maximizing the temperature drop across the TE device and the efficiency of the energy harvesting system. When the heat input is off peak, the thermal resistance is increased to dominate the thermal resistances in the system, forcing energy storage in the heat source, thus causing an increase in a source temperature. In this state very little heat ideally flows through the TE device. Once the source temperature reaches the maximum operating temperature, the thermal resistance of the switch is once again minimized. This sequence of events repeats to allow greater work to be extracted from the system by restricting heat to flow through the TE device.

In a previous study, a finite difference analytical approach with source temperature feedback was used to evaluate the potential of source temperature modulation with a thermal switch on TE power output. The analytical model demonstrated that maximizing the exergy of the source by maximizing its temperature during off-peak heat loadings is capable of improving the time-averaged power output to power input ratio (PR) of a TE device. For ideal conditions, improved time-averaged power ratios of more than 4 times were realized. Criterion defining the operation space for power ratio improvements were developed [14].

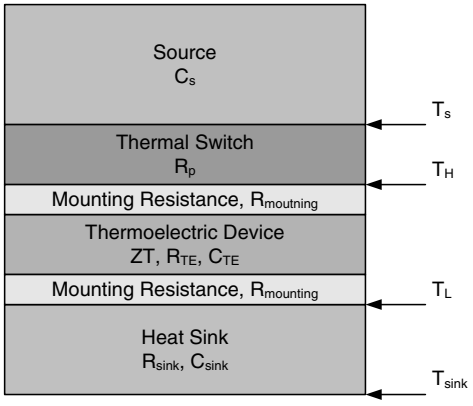

Fig. 1 Schematic of energy harvesting system with TE device and thermal switch.

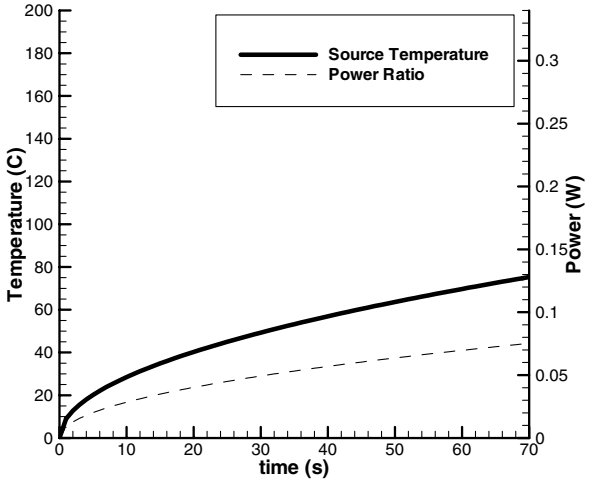

Fig. 2 Illustration of representative energy harvesting system without a thermal switch.

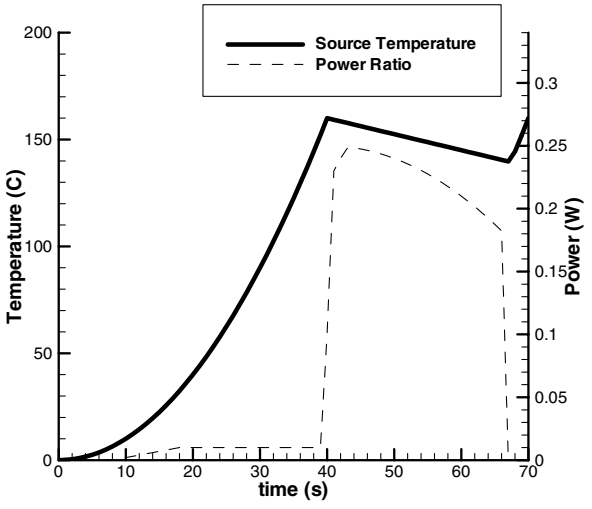

Fig. 3 Illustration of representative energy harvesting with a thermal switch.

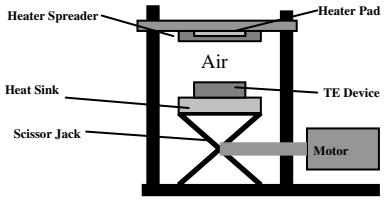

Fig. 4 Variable air gap experiment setup schematic.

II. Experiment

To experimentally investigate the effects of a thermal switch on the waste heat recovery system, an experimental setup composed serially of a fixed heat source, a variable air gap serving as a thermal switch, a thermoelectric device, and a heat sink mounted on a translation stage was employed. A schematic of this system is shown in Fig. 4. This setup consists of a fixed heat source ($1\frac{1}{2}$ in. silicon heater pad) attached to an aluminum or copper heat spreader to simulate waste heat. This heat source assembly is mounted to a fixed plate located above a lower assembly that rests on a scissor jack driven by a stepper motor thereby permitting the lower assembly to be traversed up and down. Resting on top of the scissor jack, the TE device (Hi-Z HZ-2 thermoelectric module with ceramic plates) is sandwiched between heat flux sensors and thermocouples. The heat sink, which is constructed of a copper plate with embedded tubing connected to a cooling bath pumping a 70/30 mixture of glycol to distilled water near −20°C, rests on top of the scissor jack. To represent the thermal switch in the high thermal resistance state, the stepper motor drives the scissor jack down until a desired air gap distance of 8 mm is achieved. The 8 mm gap was chosen to minimize the heat transfer from the heat source and the TE device during open conditions. Distances greater than 8 mm showed little heat transfer benefit, and distances below 8 mm had notably increased heat transfer. Thus the high thermal resistance state is associated with conduction, radiation, and convection across the air gap. To represent the thermal switch in the low thermal resistance setting, the stepper motor drives the scissor jack up until the TE device is firmly pressed against the heat source assembly. When closed, the low thermal resistance between the heater assembly and the TE device is dominated by the contact resistance between the TE device and heater spreader. Gentle pressure between the heat source and TE device, achieved by application of a weight atop the "floating" heat source, ensures adequate thermal contact between the heater spreader and TE device.

The goal of this investigation is to determine the improvement of time-averaged overall TE device power output to power input ratio (PR) for a waste heat recovery system with a thermal switch and compare it to a similar system without a thermal switch. The power ratio for the system (PR) is defined as the ratio of time-averaged power generated by the TE device to the power into the system in the form of heat from the source as shown by Eq. (3):

$$PR = \frac{P_{\text{out}}}{P_{\text{in}}} = \frac{\int_0^T W_{\text{out}}(t)\,\mathrm{d}t}{\int_0^T W_{\text{in}}(t)\,\mathrm{d}t} \tag{3}$$

The power ratio improvement due to switching is given by Eq. (4):

$$PR\,\text{Improvement} = \frac{PR_{\text{switching}} - PR_{\text{nc}}}{PR_{\text{nc}}} \tag{4}$$

Experiments were conducted for both constant heat and variable heat input. For the constant heat input tests, once the circulator (heat sink) reached a constant temperature, the silicon rubber heater pad (heat source, Q_{in}) was set to a constant power setting to ensure that the source temperature with no thermal switching was 119 ± 1.0°C at the low thermal resistance setting. The air gap was set to zero guaranteeing firm contact between the heater assembly and the TE device. In this condition, the system achieved steady state (±0.1°C) before recording data to establish the system performance for no switching. Once this baseline was established, switching was employed by opening the air gap to a distance of 8 mm and monitoring the source temperature. Once the source temperature reached 160 ± 1.0°C, the gap was once again zeroed. When the source temperature reached the lower bound, defined as $T_{s,\max} - \Delta T_s$, the air gap was again set to 8 mm and the process was repeated. The output power from the TE device was sampled every 1 s and the overall power ratio, PR, was calculated.

The variable heat input test began by determining the baseline, no control data set for a heat input described by Eq. (5):

$$Q_{\text{in}} = \frac{Q_{\max}}{2}\left[1 + \sin\left(\frac{f}{2\pi}t\right)\right] \tag{5}$$

where $Q_{\max}$ was always set to 44 W and the frequency f was varied for each test. After the baseline was established, switching was employed as described above in the constant heat input test procedures. For both constant and variable heat input tests, all temperatures and voltages were recorded using an HP E1421B data acquisition system and were sampled every second.

III. Experimental Results

A. Constant Heat Input

For the constant heat input test, the ratio between the maximum source temperature for switching and the steady-state source temperature (no switching) was maintained at 1.333°C by adjusting the heat input to the system. This ratio was set to mirror a safety factor built into a design of a thermal management system.

The thermal resistances, capacitances, temperatures, and thermoelectric properties were kept constant throughout the constant heat source test as summarized in Table 1. Three source thermal capacitances were tested to determine the effects of source thermal capacitance on power ratio improvements. For each source capacitance tested, several different source temperature ranges, $T_{s,\max} < T_s < T_{s,\max} - \Delta T_s$, were considered in an effort to find the ΔT_s for each particular source capacitance which resulted in the greatest output power ratio for energy harvested.

The mounting resistance R_{mounting} of the TE device was determined experimentally and includes the epoxy and ceramic plates used to mount the TE device to the experimental setup and contact resistance.

Figure 5 shows a plot of output power ratio improvement as a function of source temperature for the three source capacitances tested. As can be seen from the figure, an optimal ΔT_s exists for each source capacitance considered. If the ΔT_s value is too small, the time that the source is in contact with the TE device and energy is being harvested, t_{on}, is small in comparison to the time the source is not in contact with the TE device (no energy harvested), t_{off}, as seen in Fig. 6. If ΔT_s is too large, the source temperature drops to the point of degrading the output power of the TE device, as is observable in Fig. 7.

Table 2 shows the results for the optimal ΔT_s for each source capacitance tested. As the source thermal capacitance increases relative to the TE device thermal capacitance, the output power ratio

Table 1 Physical and spatial variables that remain fixed for all constant heat input experimental cases studied

Variable	Value
C_{TE}	25 J/K
R_{TE}	2.5 K/W
$T_{s,\text{steady}}$	119 ± 1.0°C
$T_{s,\max}$	160 ± 1.0°C
T_{sink}	−18.5 ± 1.0°C
$R_{P,\text{on}}$	1.75 K/W
$R_{P,\text{off}}$	120 K/W
C_{sink}	∼∞ J/K
R_{sink}	∼0 K/W
R_{Mounting}	4.1 K/W
ZT[a]	0.72 ± 10%

[a]Krommenhoek, D., "Hi-Z HZ-2 Module ZT Value," Hi-Z Corporation (private communication) [retrieved Nov. 2006].

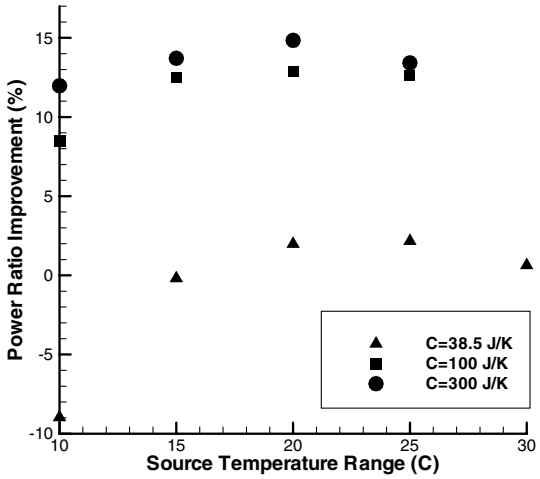

Fig. 5 Power output ratio improvements for constant heat input and $C_s = 38.5$, 100, and 300 J/K as a function of ΔT_s.

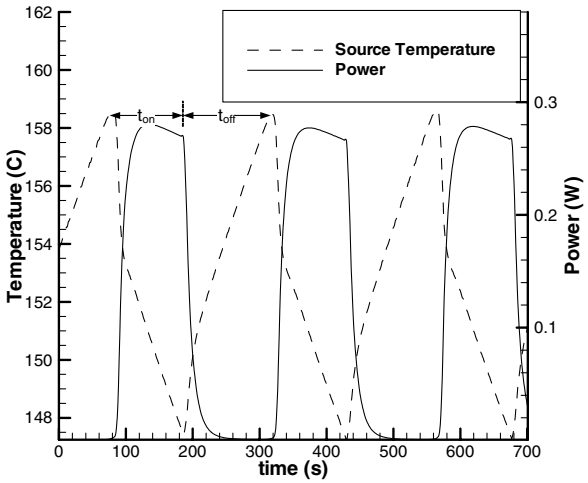

Fig. 6 Source temperature and TE output power for case 2 with $C_s = 100$ J/K, and $\Delta T_s = 10$°C.

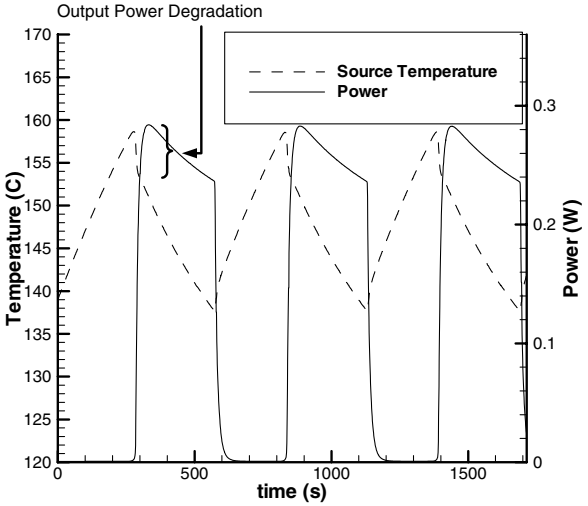

Fig. 7 Source temperature and TE output power for case 2 with $C_s = 100$ J/K, $\Delta T_s = 25$°C.

improvement increases. Larger source capacitances allow the source to store more thermal energy when the thermal switch resistance is high. When the thermal switch resistance is low, more thermal energy can be forced through the system. When the thermal capacitance of the TE device is small in comparison to the source, relatively little energy is stored in the TE device, and thus the heat dissipated from the TE device when the thermal switch is off (at lower average temperature differences) is relatively small. The ratio of source contact time with the TE device, t_{on}, divided by the time the source is not in contact with the TE device, t_{off}, at optimal ΔT_s conditions is given as t_{on}/t_{off}. In all cases, for the experiments conducted the optimal on time versus off time ratio is about 1. This result is not a general rule, but a function of the experimental conditions. Experimental uncertainty of time-averaged power ratio improvement for the system was determined to be ±0.96% and is reflected in the *PR* measurements. Also from Table 2, the power ratios for both the no control and switching cases are extremely low, on the order of 1–2%. Though these measured values are low, they are calculated from voltages and currents that range from 0.05–1.4 V and 0.01–0.3 A, respectively, well within the resolution of the measurement instruments.

Table 2 Summary of the optimal experimental power output ratio improvements for constant heat input and variable source capacitance

Case	1	2	3
Q_{in}, W	27	27	32.7
C_S, J/K	38.5	100	300
$\Delta T_{s,opt}$, °C	25	20	20
t_{on}/t_{off}	1.01	1.07	1.01
PR_{nc}, %	1.2 ± 0.33	1.4 ± 0.33	1.7 ± 0.33
Max $PR_{switching}$, %	1.2 ± 0.33	1.6 ± 0.33	1.9 ± 0.33
Max *PR* improvement, %	2.2 ± 0.96	12.9 ± 0.96	14.8 ± 0.96

Table 3 Physical and spatial variables that remain fixed for all variable input experimental cases studied

Variable	Value
Q_{max}	44 W
C_S	100 J/K
C_{TE}	25 J/K
R_{TE}	2.5 K/W
$T_{s,max}$	160 ± 1.0°C
T_{sink}	−18.8 ± 1.0°C
$R_{P,on}$	1.75 K/W
$R_{P,off}$	120 K/W
C_{sink}	∼∞ J/K
R_{sink}	∼0 K/W
$R_{Mounting}$	4.1 K/W
ZT	0.72 ± 10%

B. Variable Heat Input

For the variable heat input tests, the heat source capacitance was constant for all cases but the sinusoidal heat source input frequency was varied. Table 3 shows the fixed thermal resistances, capacitances, temperatures, and thermoelectric properties for these tests. The frequency was changed from 0.003 to 0.0003 Hz to better understand the effects of heat input frequency on power ratio improvements.

To find the optimal output power ratio at each thermal load frequency, ΔT_s was varied until a maximum power improvement

Table 4 Summary of the experimental power output ratio improvements for variable heat input

Case	1	2	3
f, Hz	0.00333	0.00056	0.00028
$T_{s,max,nc}$, °C	102	130.6	150.8
$\Delta T_{s,opt}$, °C	20	20	30
t_{on}/t_{off}	0.472	0.517	0.630
Avenue PR_{nc}, %	1.3 ± 0.33	1.4 ± 0.33	1.4 ± 0.33
Max. avenue $PR_{switching}$, %	1.6 ± 0.33	1.8 ± 0.33	1.8 ± 0.33
PR improvement, %	20.0 ± 0.96	30.0 ± 0.96	25.8 ± 0.96

ratio was determined. As can be seen from Table 4, as the frequency decreases, the maximum source temperature without control, $T_{s,\max,nc}$, increases. Additionally, the output power ratio improvement was best in case 2 for a frequency of 0.000556 Hz and $\Delta T_s = 20°C$. In case 1, the high frequency heat input prevented the heat source from fully reaching its maximum value; therefore the power ratio improvement is degraded. In case 3, the frequency is low enough that the non-negligible energy stored in the TE device is lost during open switch conditions. This heat dissipation from the TE device during this period is associated with an effectively low temperature drop across the TE device, thus degrading the time-averaged power ratio improvement. One can conclude that the optimal frequency for energy harvesting for transient heat input would depend on the thermal capacitances of the source, TE device, and the sink. If the thermal capacitance of the TE device is negligible, lower frequencies would produce more beneficial results with thermal switching.

IV. Analysis

Building upon previous work of McCarty et al. [14], a finite difference thermal *RC* equivalent model of the TE energy recovery system, shown schematically in Fig. 1, was employed and can be compared with experimental results. Conservation of energy is applied to each of the subelements:

$$\text{Source}: \frac{dT_s}{dt} = \frac{1}{C_s}[Q_{in}(t) - Q_{out}] \tag{6a}$$

Here Q_{in} and Q_{out} are, respectively, the heat dissipation by the source and the heat leaving the source and passing either into the TE device (for the baseline case) and into the thermal switch otherwise:

$$\text{Thermal switch}: \frac{dT_p}{dt} = \frac{1}{C_p}\left[k_p \frac{\partial^2 T_p}{\partial x^2}\right] \tag{6b}$$

$$\text{Sink heat exchanger}: \frac{dT_{sink}}{dt} = \frac{1}{C_{sink}}\left[k_{sink} \frac{\partial^2 T_{sink}}{\partial x^2}\right] \tag{6c}$$

Finally, for the TE device, the quasisteady assumption permits determination of the TE energy recovery efficiency from the hot side and cold side TE temperatures from Eq. (6) [15]:

$$\eta = \frac{P_{out}}{Q_{in}} = \frac{T_{TE,H} - T_{TE,L}}{T_{TE,H}} \left(\frac{\sqrt{1+ZT}-1}{\sqrt{1+ZT}+\frac{T_{TE,L}}{T_{TE,H}}}\right) \tag{7}$$

The boundary conditions employed for these elements are continuity of heat flow and temperature at each interface. For convenience all temperatures are initially set equal to the sink temperature T_{sink}.

The physical model given by Eqs. (6) and the specified boundary and initial conditions are evaluated using a finite difference formulation. The ultimate aim of this formulation is to evaluate the time-averaged TE output power ratio shown in Eq. (3).

Using this finite difference model, the following thermal resistances, capacitances, temperatures, and thermoelectric properties were kept constant throughout the constant heat source simulation, in an effort to represent the experimental setup conditions, as shown in Table 5.

The finite difference model was used to predict the behavior of the waste heat recovery system with three different heat source thermal capacitances. The heat input Q_{in} was adjusted until the steady-state source temperature was $119 \pm 1.0°C$. For each case studied, ΔT_s was varied until a maximum power ratio was determined analytically.

Table 6 shows the results for the analytical model with constant heat input. The ratio of the source contact time, t_{on}/t_{off}, was slightly different for the analytical model due to the differences in experimental heat losses of the system. In both the analytical model and experiment results, the power ratio improvements increased as the thermal capacitance of the source increased. Although the magnitude of the improvement is different, the trends were consistent.

Table 5 Physical and spatial variables that remain fixed for all constant heat input simulated cases studied

Variable	Value
C_{TE}	25 J/K
R_{TE}	2.5 K/W
$T_{s,steady}$	118.8°C
$T_{s,max}$	160°C
T_{sink}	−20°C
$R_{P,on}$	1.75 K/W
$R_{P,off}$	120 K/W
C_{sink}	100,000 J/K
R_{sink}	0.0005 K/W
$R_{Mounting}$	4.1 K/W
ZT	0.72

Table 6 Summary of simulated and experimental power output ratio improvements for constant heat input

Case	1	2	3
C_S, J/K	38.5	100	300
ΔT_s, °C	30	25	20
t_{on}/t_{off}	1.14	1.5	2.5
Analytical *PR* Imp, %	4.6	13.1	26.8
Exp. *PR* Imp, %	2.2 ± 0.96	12.9 ± 0.96	14.8 ± 0.96

V. Capacitance Effects

For the constant heat input experiments, it was noticed that as the source thermal capacitance increased at constant TE thermal capacitance, the output power ratio increased for both the experiment and finite difference simulation. To further investigate this phenomenon, the effect of different capacitance ratios, defined as the source thermal capacitance divided by the TE device thermal capacitance, on power output ratio was investigated both analytically and experimentally. As can be seen from Fig. 8, increasing the capacitance ratio increases the output power ratio of the system with thermal switch control. Notably, when the thermal capacitance of the TE device is greater than the source, controlled thermal switching has no beneficial effect. For this case, heat transfer to the TE device causes significant thermal energy storage in the TE device. Thus, when the thermal resistance of the thermal switch is high, the thermal energy storage in the TE device is released at a smaller effective

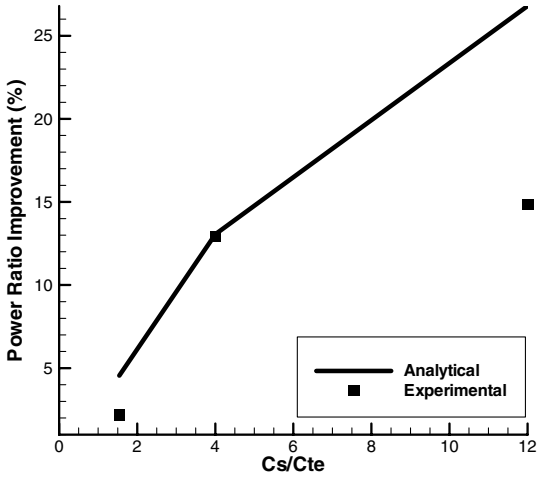

Fig. 8 Finite difference model and experimental power output ratio improvements as a function of thermal capacitance ratio.

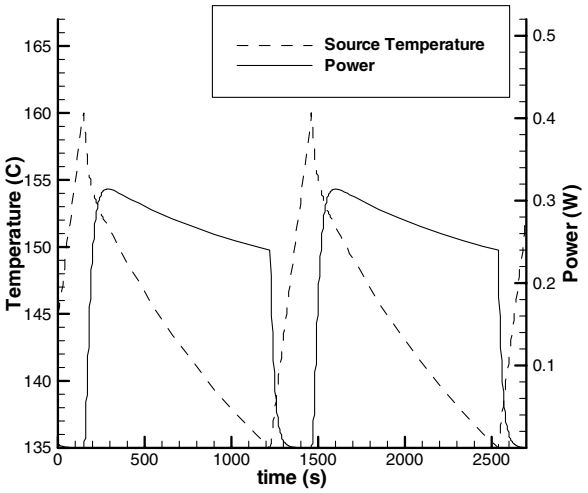

a)

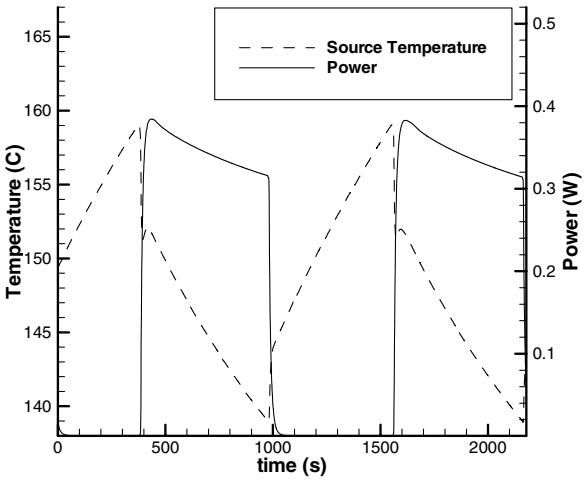

b)

Fig. 9 a) Finite difference results for constant heat input for case 3, $Q_{\text{in}} = 32.7$ W, $C_s = 300$ J/K, and $T_{s,\max} = 160°$C. b) Experimental results for constant heat input results for case 3, $Q_{\text{in}} = 32.7$ W, $C_s = 300$ J/K, and $T_{s,\max} = 160°$C.

temperature drop across the device thus reducing overall performance. Therefore the source thermal capacitance must be greater than the TE device thermal capacitance in order for thermal switching to be beneficial in waste heat recovery systems. This high thermal capacitance ratio could be realized in practice with thin-film superlatice TE devices.

VI. Comparison Between Model and Experimental Results

A plot of the source temperature and TE output power for the finite difference model with constant heat input is shown in Fig. 9a. A similar plot with the experimental data is shown in Fig. 9b. These plots for both the finite difference model and experiment for comparable input parameters are very similar. In fact, both the analytical model and experiment required a heat input of 32.7 W to achieve the required steady-state temperature of 119°C in the low thermal resistance setting. The finite difference model shows a maximum power ratio of 0.7%, with overall power improvement ratios increased by 26.8%. The maximum power ratio of the experimental system was 1.9%, with overall power improvement ratios increased by 14.8%. The greatest difference between the analytical and experimental results was at the highest source capacitance, where heat losses to the environment were largest and not accounted for in the analytical model. Thus the analytical results overestimate the experimental measurements.

VII. Projected Results for State-of-the-Art TE Device

Although the *PR* improvements in the previous sections were notable, the overall efficiencies were still low because of the mounting resistance of the TE used in the experiment. To better understand the effects of thermal switching for waste heat recovery systems with state-of-the-art TE devices, results for a state-of-the-art TE device can be projected using the experimentally verified analytical model. For a waste heat recovery system operating at a maximum source temperature of 160°C, a source capacitance of 100 J/K, a TE capacitance of 1 J/K, a ZT of 3, and minimal mounting resistance and heat loss, the overall power output ratio could improve to more than 35% with a thermal switch as predicted by the finite difference model.

VIII. Conclusions

Both constant and variable heat inputs were tested experimentally using the variable air gap setup. For constant heat input, several different heat source capacitances were considered. The sensitivity of changes in these parameters on the time-averaged efficiency was determined. For the variable heat input, several different heat input frequencies were also evaluated. Experimental power ratios for constant heat input improved up to 15% and for variable heat input improved up to 30% in certain design space conditions.

The experimental results provided in this paper prove that thermal switching can improve the performance of waste heat recovery systems on unmanned air vehicles that use TE devices. Also, the source thermal capacitance must be greater than the thermal capacitance of the TE device for thermal switching to improve output power recovered from a waste heat recovery system. Additionally, the experimental results verified the effectiveness of the analytical finite difference model developed in previous work. Finally, the analytical model predicted that thermal switching could boast a state-of-the-art waste heat recovery system output power ratio by 35% for constant heat input in certain design space conditions.

Acknowledgments

We would like to thank the Dayton Area Graduate Studies Institute and the Air Force Office of Scientific Research for their continued funding and support and Hi-Z for the donation of the TE devices.

References

[1] Chen, G., *Nanoscale Energy Transport and Conversion*, Oxford University Press, Oxford, England, U.K., 2005, pp. 254–391.

[2] Dresselhaus, M. S., Lin, Y. M., Black, M. R., Rabin, O., and Dresselhaus, G., "New Directions for Low Dimensional Thermoelectricity," *Materials Research Society Symposium Proceedings*, Materials Research Society, Pittsburgh,2003, pp. 419–430.

[3] Venkatasubramanian, R., Viivola, E., Calpitts, T., and O'Quinn, B., "Thin Film Thermoelectric Devices with High Room Temperature Figures of Merit," *Nature (London)*, Vol. 413, No. 6856, Oct. 2001, pp. 597–602.

[4] Martin, P. M., and Olsen, L. C., "Recent Progress in Scale Up of Multilayer Thermoelectric Films," *DOE/EPRI High Efficiency Thermoelectrics Workshop*, Materials Research Society, San Francisco, 17–20 Feb. 2004.

[5] Bell, L., "Thermoelectric Technology Readiness for Large Scale Commercialization," *DOE/EPRI High Efficiency Thermoelectrics Workshop*, Materials Research Society, San Francisco, 17–20 Feb. 2004.

[6] Fairbanks, J., "Chair's Overview of High Efficiency Thermoelectrics and Potential," *DOE/EPRI High Efficiency Thermoelectrics Workshop*, Materials Research Society, San Francisco, 17–20 Feb. 2004.

[7] Elder, A., Bertram, M., and Liebl, J., "Visions of Possible Thermoelectrics for Vehicle Applications," *DOE/EPRI High Efficiency Thermoelectrics Workshop*, Materials Research Society, San Francisco, 17–20 Feb. 2004.

[8] Hallinan, K. P., and Sanders, B., "Entropy Generation Metric for Evaluating and Forecasting Aircraft Energy Management Systems," *International Journal of Exergy*, Vol. 2, No. 2, 2005, pp. 120–145.

[9] Hoyos, G. E., Rao, K. R., and Jerger, D., "Fast Transient Response of Novel Peltier Junction," *Energy Conversion*, Vol. 17, No. 1, 1977, pp. 45–54.

[10] Stilbans, L. S., and Fedorovich, N. A., "The Operation of Thermoelectric Elements in Non-Stationary Conditions," *Soviet Physics Technical Physics*, Vol. 3, 1958, pp. 460–462.

[11] Landecker, K., and Findlay, A. W., "Study of the Fast Transient Behavior of Peltier Junctions," *Solid-State Electronics*, Vol. 3, No. 3, 1961, pp. 239–260.

[12] Idnurm, M., and Landecker, K., "Experiments with Peltier Junctions Pulsed with High Transient Currents," *Journal of Applied Physics*, Vol. 34, No. 6, 2004, pp. 1806–1810.

[13] Gray, P. E., "Approximate Dynamics Response Calculations for Thermoelectric Peltier-Effect Devices," *Solid-State Electronics*, Vol. 6, 1963, pp. 339–348.

[14] McCarty, R. et al., "Enhancing Thermoelectric Energy Recovery via Modulations of Source Temperature for Cyclical Heat Loadings," *Proceedings of ASME InterPack'05*, ASME, New York, 2005.

[15] Goldsmid, H. J., "Conversion Efficiency and Figure-of-Merit," *CRC Handbook of Thermoelectrics*, CRC Press, Boca Raton, 1994, pp. 19–25.